

The Effect of Punch Tilting in Evaluating Powder Densification in a Rotary Tablet Machine

MARCO CESPI,¹ MONICA MISICI-FALZI,¹ GIULIA BONACUCINA,¹ SARA RONCHI,²
GIOVANNI F. PALMIERI¹

¹Department of Chemical Sciences, University of Camerino, Via S. Agostino 1, I-62032 Camerino (MC), Italy

²Ronchi Tablet Machines and Toolings (www.officineronchi.it), Via Pavia 42/44, 20053 Muggiò (MI), Italy

Received 22 January 2007; revised 29 March 2007; accepted 30 March 2007

Published online in Wiley InterScience (www.interscience.wiley.com). DOI 10.1002/jps.21030

ABSTRACT: The effect of punch tilting on the mechanism of punch penetration in the die of a rotary tablet machine during the compression cycle was evaluated by installing four displacement transducers on one station of a rotary machine. Two transducers were symmetrically positioned beside the upper punch in the upper turret, and the other two transducers were similarly placed beside the lower punch in the lower turret. Microcrystalline cellulose and dicalcium phosphate dihydrate were compressed at 5, 10, 15 and 20 kN using two different machine speeds, in order to quantify the effect of punch tilting in the evaluation of punch penetration. These compression data served to construct the powder bed reduction curves, from which it was possible to establish that punch tilting is directly proportional to the compression force used. Tilting is maximal at the beginning of the dwell time, disappears at half dwell time, and reaches a new maximum at the end of the dwell time. In latter case, tilting occurred in the direction opposite that of the first maximum. The impact of tilting in powder densification behaviour, evaluated through the construction of Heckel plots, depends on the compression force used in the analysis. Heckel plots are as distorted as the compression force is elevated. Consequently, the calculated Heckel parameters differ from the real values. Unless a very low compression force is used, a proper Heckel analysis can be performed in a rotary machine only if it is fitted with a device that includes the effect of punch tilting in the evaluation of punch penetration. © 2007 Wiley-Liss, Inc. and the American Pharmacists Association *J Pharm Sci* 97:1277–1284, 2008

Keywords: compression; rotary machine; punch tilting; Heckel plot

INTRODUCTION

Tablets are the most common pharmaceutical dosage form, but while the compression of powdered or granular material into a cohesive

mass may seem simple, it is actually a complex and irreversible dynamic process.

Mechanically, the process consists of imposing a progressive strain on the powder, confining it to a certain final volume and porosity.

The dimensional constraints imposed by the punches and die are then removed and the compact is allowed to relax.

The compacted material exerts a certain stress against the punches and die during this process in response to the imposed strain.

Correspondence to: Giovanni F. Palmieri (Telephone: 0737/402289; Fax: 0737/637345; E-mail: gianfilippo.palmieri@unicam.it)

Journal of Pharmaceutical Sciences, Vol. 97, 1277–1284 (2008)
© 2007 Wiley-Liss, Inc. and the American Pharmacists Association

Knowledge of the mechanism of powder densification in the die is fundamental for optimising tablet formulation at a very early stage of product development; with this information, requirements for achieving a robust tablet composition and avoiding scale-up and production problems such as capping or insufficient crushing strength can be predicted.

Useful information concerning powder densification can be drawn from compression stress/strain data, and a great deal of research has been devoted to developing methods of evaluation based on these data, so that the formation of the compact and its subsequent behaviour under stress inside the die of a tablet machine can be monitored.

Two such widely used methods include force/displacement curves, first proposed by Nelson,¹ which allow evaluation of energy expenditure during powder compaction, and Heckel's plot of the negative logarithm of tablet porosity versus compression pressure,²⁻³ which has recently become the most used because it provides a good level of information about the dynamics of powder densification in the die.

The Heckel equation is:

$$\ln \frac{1}{1-D} = KP + A$$

where D is the relative density and $(1-D)$ denotes the pore fraction, P is the applied pressure, K is the slope of the straight linear portion of the plot and the reciprocal of K is the mean yield pressure (P_Y), A is the intercept of the prolonged linear portion of the plot with the Y axis and is the sum of two densification terms:

$$A = \ln \frac{1}{1-D_0} + B$$

where D_0 is the initial relative density and B is the densification due to the slippage and rearrangement of primary and fragmented particles.

So, the relative density at point A is $D_A = 1 - e^{-A}$ and the increase of relative density due to slippage and rearrangement is $D_B = D_A - D_0$.

The use of this method requires measuring the force as it varies during the punch penetration inside the die. Of course, the accuracy and resolution of the devices used to collect these types of data is essential.

Single station eccentric presses are usually employed to acquire the stress/strain data. In fact, in this type of machine, only the upper punch moves vertically and penetrates the die to

compress the material, whilst the position of the lower punch remains unchanged (except for deflection) during the tablet formation. For this reason, eccentric presses can be easily instrumented to measure the axial forces exerted by both punches and the distance moved by the upper punch.

Compaction simulators also represent a powerful means for collecting these data, particularly when material characterisation is needed, since they can reproduce different compression kinetics.⁴⁻⁶

Recently, acquisition of compression cycle stress/strain data has been made possible even for rotary tablets machines. In a previous work, the authors mounted two displacement transducers in the turrets beside the upper and lower punches in one of the 10 stations of a Ronchi rotary tablet machine, thus enabling a direct comparison between the Heckel plots obtained from the eccentric and the rotary machine.⁷ Transducers were mounted very close to the punches and 6 mm diameter flat faced punches were used in order to minimise any possible punch tilting phenomena.

The deformation of the rotary machine and its effect on the construction of the Heckel plot was pointed out, though a concomitant little effect of punch tilting could not be excluded.⁷

Another work⁸ demonstrated by using a partially modified portable device and compressing a flat steel tablet that punch tilting influences the correct value of punch displacement; the authors suggested minimising or correcting this phenomenon with the use of two transducers per punch for precise measurement of punch displacement.⁸

The aim of this work was to investigate the extent of punch tilting that occurs in a rotary machine under dynamic conditions, the parameters that could affect the tilting, and its specific effect on the Heckel plot profile. The latter aspect is of the most interest, since it gives a direct idea about the real possibility of performing a Heckel analysis using a rotary machine.

Thus, common materials for direct compression were used and the experimental conditions were such that punch tilting was allowed to occur.

MATERIALS AND METHODS

Punch Displacement Device

One of the eight stations of a Ronchi FA rotary tablet machine was equipped with four LVDT

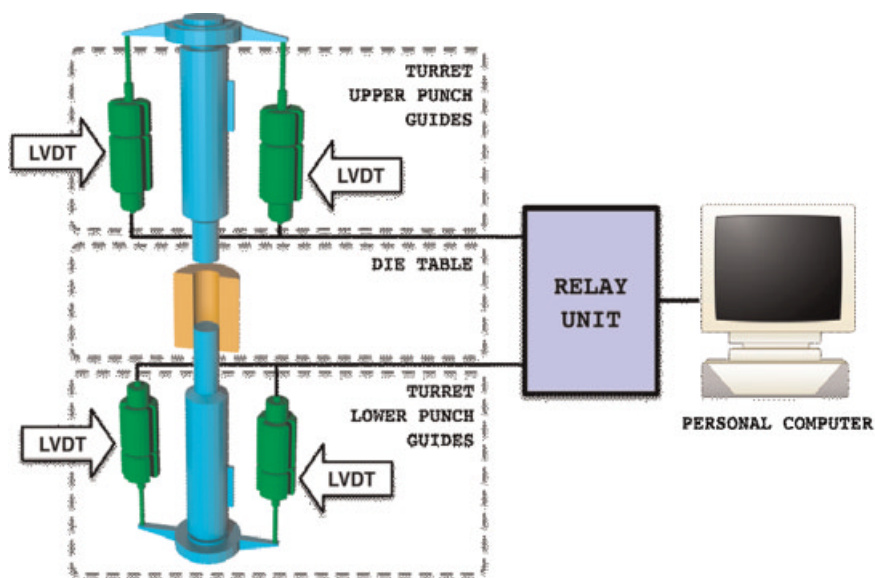


Figure 1. Device for punch displacement control.

transducers. They were symmetrically installed beside the punches (one preceding and one succeeding) in either the upper or the lower turrets, according to the chart in Figure 1. Punches were equipped immediately below their head, with two symmetrical narrow flat steel arms that ended just above the transducer. The remaining seven stations were blinded.

Displacement Transducer Set Up

Transducer calibration and validation were performed by the Ronchi Company using both a micrometer screw and international standard blocks (Mitutoyo, Tokyo, Japan). Calibration was performed when punches were not in contact with rollers or slope guides in order to avoid the cancellation of any basic tilting. Zero penetration for the lower punch was set at the minimal punch penetration position inside the die. Zero penetration for the upper punch was set as the contact point between the punch and a blind steel die at zero force.

Compression Data Acquisition

Microcrystalline cellulose (Avicel PH 102) and dicalcium phosphate dihydrate (Emcompress) were compressed with 11.28 mm flat-faced punches, by manually introducing the powder into the prelubricated die (magnesium stearate slurry in acetone), after having adjusted the weight of the samples in order to obtain the desir-

ed pressure. Punch penetration was not changed once fixed. Five replicates cycles were performed for the two materials at maximal force of 5, 10, 15, 20 kN and compression speed of 10 and 25 rpm. Five replicate cycles were also performed at 0 kN (empty die) without changing punch penetration.

For a single compression cycle, the compression force and the displacement of the upper and lower punches were measured and recorded at a frequency of 400 Hz by both the preceding and succeeding transducers as independent signals.

Correction of the displacement transducer data for machine looseness was not necessary since the transducers position in the turrets (Fig. 1) enabled the automatic detection of machine deflection.

The correction of punch deformation was carried out point by point according to the following equation:

$$D = \frac{FL}{ES}$$

where D is the punch deformation (mm), F is the applied force (kN), L is the punch length (mm), E is the steel rigidity modulus (kN/mm²), and S is the punch section (mm²).

The equation is valid below the limit of steel elasticity, which is by far higher than the pressures used to perform the analyses. In addition, for a more precise correction, punch length was divided in two parts: punch stem (25 mm diameter) and punch neck (11.28 mm diameter).

Processing of Force/Displacement Data

Plots of powder bed reduction against time were generated for a compression cycle (the time between the appearance and disappearance of a compression force) using signals deriving from either the preceding or succeeding displacement transducers. For this reason, they will henceforth be referred to as the preceding plot and succeeding plot. A mean powder bed reduction plot was then constructed as the average of the preceding and succeeding displacement values.

The maximal difference between the preceding and succeeding plots and its position over the time was then considered.

Heckel profiles (in die method) were then generated from single compression cycles by using data of either the preceding or succeeding powder bed reduction plot. A mean Heckel plot was then obtained from data of the mean powder bed reduction plot. D_A , D'_0 , and D'_B were calculated for all the plots. D'_0 allows a distinction between densification due to the movement of the original particles and that due to the brittle fracture, since it is calculated using the last relative density before the appearance of a pressure. D'_0 term includes the initial rearrangement of particles.⁹ Therefore, D'_B can be calculated as $D'_B = D_A - D'_0$ and is only representative of the densification due to fragmentation.

P_Y was calculated from the right portion of the plots, before the deviation between the preceding and succeeding plots.

The immediate elastic recovery E_R was also calculated according to the following equation:

$$E_R = \frac{D_{\max} - D_{\text{fin}}}{D_{\max}} 100$$

where the maximal relative density (D_{\max}) during the compression cycle was calculated as the point of minimal distance between upper and lower punches.

Relative density at the end of the compression cycle (D_{fin}) was calculated from the last point of the decompression portion of the curve.

RESULTS AND DISCUSSION

Powder Bed Reduction and Punch Tilting

Figure 2 shows a plot of bed reduction inside the die without any material in it.

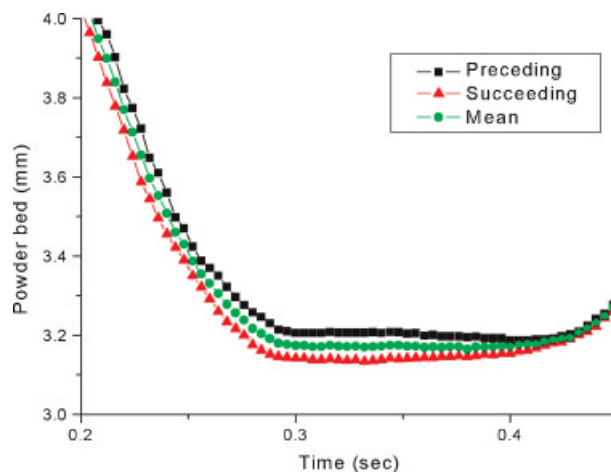


Figure 2. Bed reduction of an empty die during punches penetration as assessed by the preceding and succeeding transducers, and the mean of both signals (10 rpm).

As can be noted, there is a small difference between the preceding and succeeding curves and this, of course, depends on the signals retrieved from the preceding and succeeding transducers. As expected because of the mechanism of punch tilting, both signals are incorrect. Values of punch penetration from the preceding transducers are underestimated, whilst values from the succeeding transducers are overestimated.

This small difference (40 μm) is more or less constant until the beginning of the dwell time, when it diminishes slowly but progressively during the dwell time itself. At the end of the dwell time, the two signals are practically identical. In fact, at the end of the dwell time, the contact between punch and roller ceases and the friction responsible for the difference in the punch displacement values is no longer present.

The interval of time reported in Figure 2 does not exactly correspond to the compression cycle obtained with a full die but is shorter; the Y axis has been expanded in order to show this basic small difference.

When a powder material is present in the die, for instance Avicel PH 102, the trend of both the preceding and succeeding curves of powder bed reduction changes, particularly in proximity to the dwell time (Fig. 3).

The underestimation of punch penetration values obtained from the preceding transducers and the overestimation from the succeeding transducers increase considerably and symmetrically because of the resistance given by the material in the die.

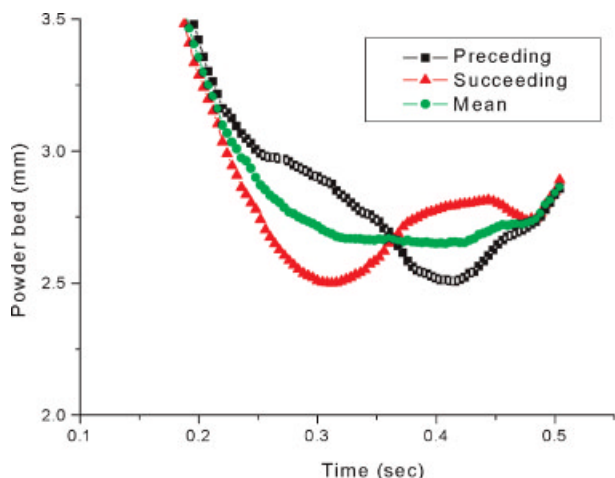


Figure 3. Preceding, succeeding and mean powder bed reduction curves obtained at the maximal compression force of 20 kN and 10 rpm (200 MPa pressure).

After having reached a maximum, this deviation from the real estimation of punch penetration reduces gradually until disappearing at a given time, but then it increases anew until reaching another maximum, before definitively disappearing, in agreement with previously reported data.⁸

After this cross over between the preceding and succeeding curves, the deviation from the real estimation is inverted. Punch penetration is overestimated by the preceding transducers and underestimated by the succeeding transducers.

In all cases, the correct values of punch displacement are represented by the average between the preceding and succeeding signals (mean curve).

Table 1 reports the maximal differences between the preceding and succeeding curves (D_1 , D_2) occurring at 5, 10, 15 and 20 kN compression forces and their corresponding time of occurrence (T_1 , T_2) within the compression cycle. The extent of this maximal difference increases gradually as the compression force increases but it always occurs more or less after the same time from the beginning of the compression cycle. Of course T_1 and T_2 values change if the compression speed is changed (10–25 rpm) but if a specific speed is considered they remain more or less constant.

D_2 is always lower than D_1 but this simply depends on the fact that during the dwell time the compression force slowly diminishes.

When the D_1 and D_2 values are reported against compression force (Fig. 4) it is clearly visible that they increase linearly as the compression force increases.

Very similar results are obtained using Emcompress instead of Avicel and for this reason they are not shown.

An exhaustive explanation of the mechanism of punch tilting is afforded when the preceding, succeeding, and mean curves are reported against time, together with the compression force curve. At the same time, the position of the maximal compression force, beginning and end of the dwell time, D_1 and D_2 are highlighted (Fig. 5).

The maximal compression force occurs just a few instants before beginning of the dwell time in agreement with previously reported data.⁷ D_1 occurs very shortly after the beginning of the dwell time. In practice, all three phenomena occur at the same time. D_2 occurs a few instants after the end of the dwell time.

Table 1. Maximal Differences Between Preceding and Succeeding Curves (D) and Corresponding Time (t) of Occurrence

| | 0 kN | 5 kN | 10 kN | 15 kN | 20 kN |
|------------|-----------------|-----------------|-----------------|-----------------|-----------------|
| 10 rpm | | | | | |
| t_1 (s) | | 0.28 ± 0.01 | 0.28 ± 0.01 | 0.30 ± 0.05 | 0.29 ± 0.07 |
| D_1 (mm) | 0.04 ± 0.01 | 0.18 ± 0.02 | 0.23 ± 0.02 | 0.35 ± 0.04 | 0.42 ± 0.01 |
| t_2 (s) | | 0.41 ± 0.01 | 0.41 ± 0.01 | 0.41 ± 0.01 | 0.41 ± 0.03 |
| D_2 (mm) | | 0.17 ± 0.01 | 0.22 ± 0.01 | 0.29 ± 0.03 | 0.31 ± 0.02 |
| 25 rpm | | | | | |
| t_1 (s) | | 0.11 ± 0.04 | 0.12 ± 0.01 | 0.12 ± 0.03 | 0.12 ± 0.02 |
| D_1 (mm) | 0.04 ± 0.01 | 0.16 ± 0.02 | 0.22 ± 0.01 | 0.32 ± 0.03 | 0.41 ± 0.02 |
| t_2 (s) | | 0.17 ± 0.01 | 0.18 ± 0.02 | 0.17 ± 0.03 | 0.17 ± 0.04 |
| D_2 (mm) | | 0.14 ± 0.03 | 0.20 ± 0.03 | 0.26 ± 0.02 | 0.30 ± 0.02 |

D_1 and t_1 : first maximum before the cross over. D_2 and t_2 : second maximum after the cross over.

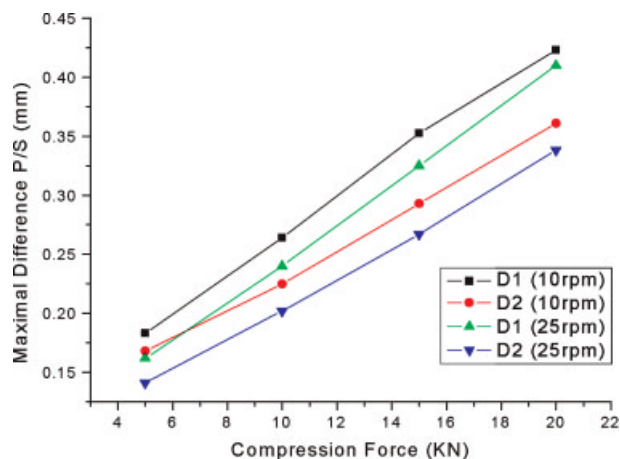


Figure 4. Variation of the maximal distances D_1 and D_2 between preceding and succeeding curves in function of the compression force.

At this point, it is clear that punch tilting depends on material resistance and is therefore absolutely proportional to compression force. In fact, as already said, the maximum tilting corresponds to the maximum compression force. D_2 occurs just after the beginning of the drastic force reduction due to the decompression phase.

The mean curve gives the correct values of powder bed reduction.

The change in tilting direction, as evidenced by the crossover between preceding and succeeding signals, occurs more or less at half dwell time,

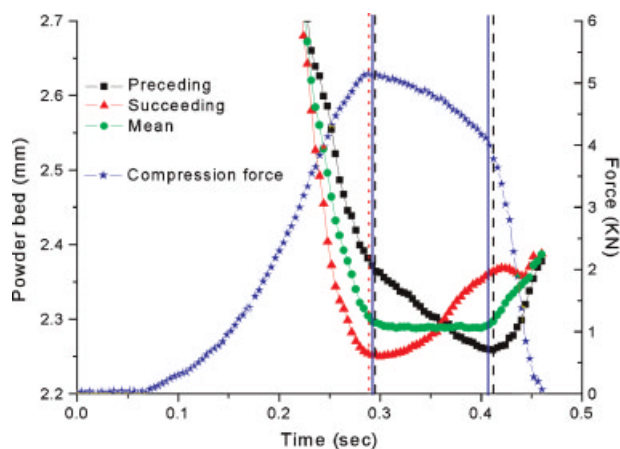


Figure 5. Relation between powder bed reduction curves (preceding, succeeding and mean), compression force and dwell time (10 rpm). Vertical solid bars indicate the beginning and end of the dwell time. The vertical short dash bar indicates the maximal compression force. Vertical dash bars indicate the maximal distances between preceding and succeeding curves (D_1 and D_2).

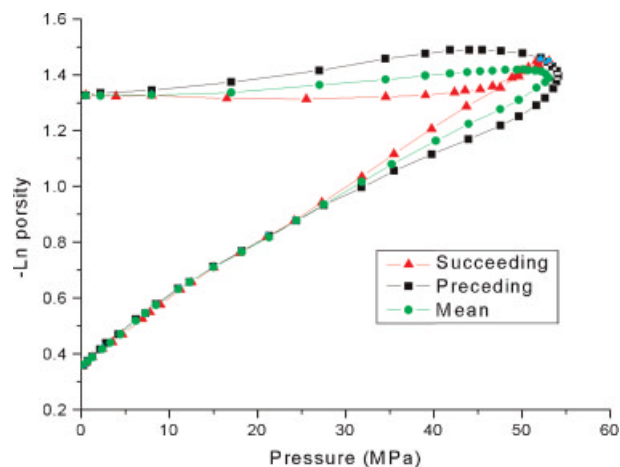


Figure 6. Heckel plot of Avicel PH 102 obtained at the maximal compression force of 5 kN (50 MPa) and 25 rpm.

when upper and lower punches are perfectly aligned below and above the respective compression rollers. After this crossover, most of the flat portion of the punch head has overcome the roller and punch tilting that occurs in the opposite direction.

Heckel Plots

The impact of punch tilting on the construction of the Heckel plot is important and cannot be neglected. It becomes more and more evident as the compression force increases.

Figures 6 and 7 show the Heckel plots for Avicel PH 102 generated from signals emitted by the

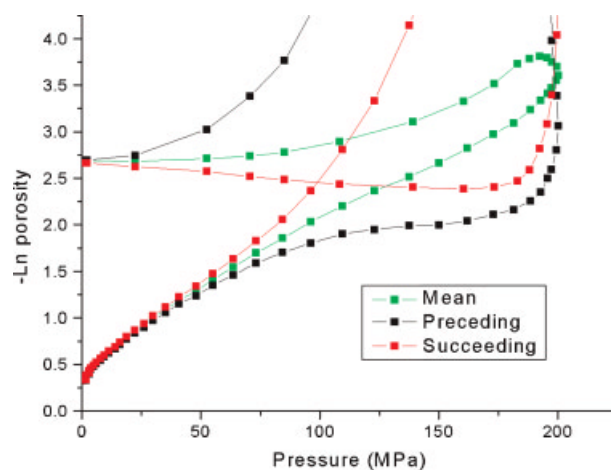


Figure 7. Heckel plot of Avicel PH 102 obtained at the maximal compression force of 20 kN (200 MPa) and 25 rpm.

Table 2. Heckel Parameters for Avicel PH 102 Obtained From the Preceding, Succeeding and Mean Heckel Plots Obtained at 25 rpm

| Compression Pressure | 50 MPa | 100 MPa | 150MPa | 200 MPa |
|----------------------|-----------------|-----------------|-----------------|-----------------|
| D'_0 | | | | |
| Preceding | 0.29 ± 0.03 | 0.30 ± 0.05 | 0.30 ± 0.06 | 0.29 ± 0.01 |
| Succeeding | 0.30 ± 0.03 | 0.30 ± 0.05 | 0.31 ± 0.08 | 0.29 ± 0.01 |
| Mean | 0.30 ± 0.03 | 0.30 ± 0.05 | 0.31 ± 0.07 | 0.29 ± 0.01 |
| D_A | | | | |
| Preceding | 0.34 ± 0.03 | 0.36 ± 0.05 | 0.38 ± 0.09 | 0.40 ± 0.06 |
| Succeeding | 0.33 ± 0.04 | 0.34 ± 0.01 | 0.37 ± 0.05 | 0.39 ± 0.01 |
| Mean | 0.34 ± 0.03 | 0.36 ± 0.03 | 0.37 ± 0.06 | 0.40 ± 0.07 |
| D'_B | | | | |
| Preceding | 0.05 ± 0.02 | 0.06 ± 0.06 | 0.07 ± 0.02 | 0.11 ± 0.04 |
| Succeeding | 0.03 ± 0.04 | 0.03 ± 0.04 | 0.05 ± 0.07 | 0.09 ± 0.07 |
| Mean | 0.04 ± 0.01 | 0.06 ± 0.08 | 0.06 ± 0.02 | 0.10 ± 0.05 |
| P_Y | | | | |
| Preceding | 55.3 ± 0.98 | 59.6 ± 1.37 | 62.3 ± 2.01 | 65.1 ± 1.34 |
| Succeeding | 49.8 ± 0.86 | 51.5 ± 1.37 | 55.8 ± 1.21 | 59.1 ± 2.79 |
| Mean | 52.7 ± 0.74 | 56.6 ± 1.09 | 59.1 ± 1.14 | 61.9 ± 1.71 |
| E_R | | | | |
| Preceding | 4.70 ± 0.06 | 5.81 ± 0.03 | 7.83 ± 0.03 | ERR |
| Succeeding | 3.46 ± 0.10 | 4.79 ± 0.02 | 7.49 ± 0.08 | ERR |
| Mean | 3.08 ± 0.07 | 3.55 ± 0.04 | 3.89 ± 0.04 | 4.15 ± 0.03 |

P_Y is calculated from data prior to the divergency among curves.

preceding and succeeding transducers. In addition, the correct trend of the Heckel plot is shown, as obtained by the mean between the preceding and succeeding data.

The divergence of both the preceding and succeeding Heckel plots from the real one is visible even when a maximal compression force of 5 kN is used, taking place after 30 MPa of pressure (Fig. 6). Thus, in practice, the first half of the ascending portion of the plot is superimposable for the three curves. Theoretically, if this first part of the plot can be used to calculate the P_Y , only one transducer per punch might be considered sufficient (Tab. 2). In practice, there is uncertainty about the beginning of this divergence if two symmetrical transducers per punch are not installed in the rotary machine. In any case, 50 MPa of pressure are not usually enough to carry out a Heckel analysis. Besides, the possibility of installing only one transducer per punch cannot be considered for materials like Emcompress, whose first portion of the ascending Heckel plot is not linear because of particle fragmentation (Fig. 8).

This divergence between preceding and succeeding Heckel plots proportionally and strongly increases as the compression force increases. In fact, when a maximal compression force of 20 kN is used (Fig. 7), except for the very first 40–45 MPa

of pressure, both the preceding and succeeding plots are completely wrong and even out of scale for a considerable part of the plot.

On the contrary, the Heckel plot obtained from the mean punch penetration values is correct and in agreement with the trend typical of a rotary machine.⁷

The end of the Heckel plot is in practice identical for the three curves (Figs. 6–8), a result that matches well with the convergence between

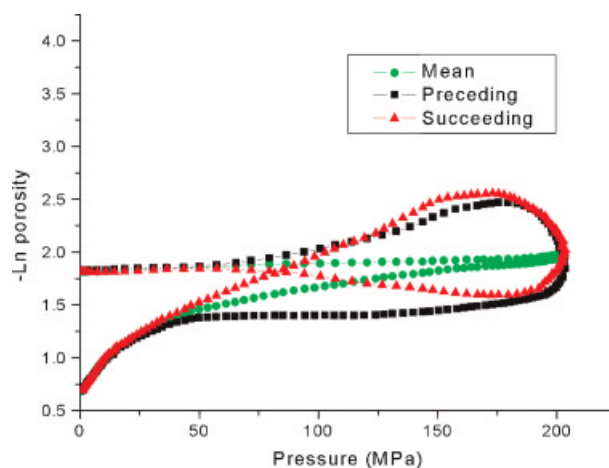


Figure 8. Heckel plot of Emcompress obtained at the maximal compression force of 20 kN (200 MPa) and 25 rpm.

preceding and succeeding signals occurring as the end of the compression cycle approaches (Fig. 5).

Heckel plots are of course in agreement with the powder bed reduction plots. Before half dwell time, the underestimation of punch penetration given by the preceding transducers corresponds to the negative deviation of the Heckel plot from the real curve, and the overestimation given by the succeeding transducers corresponds to the positive deviation of the Heckel plot. After half dwell time, the situation is inverted.

Table 2 shows as an example the Heckel parameters of the preceding, succeeding and mean curves for Avicel PH 102 (25 rpm).

As expected, D'_0 values are very similar, regardless of the type of signal used. In fact, the compression force is still zero at the values of relative density corresponding to D'_0 . This is consistent with the mechanism of punch tilting previously described.

Little variation is present in the values of D_A , D'_B and P_Y between the preceding or succeeding curve, and the mean curve (the real one), but it should not be forgotten that the linear regression was performed by using the values of the first portion of the plot, before the divergence of the curves. In any case, this initial linear portion becomes gradually shorter as the compression force increases (Figs. 6 and 7) and, as already said, is not present in fragmenting materials (Fig. 8). Thus its use is limited, risky, and inaccurate. In fact, if a little portion of the preceding or succeeding curves after their divergence is also included in the calculation of the linear regression, the results are completely wrong.

Preceding and succeeding values of elastic recovery (E_R) are always different from real values obtained from the mean curves. The difference is little only for the succeeding value at 50 MPa. In any case, preceding and succeeding values of E_R become more inaccurate when the compression force is increased. At 20 kN compression force (200 MPa pressure) these E_R values cannot be calculated, since a considerable portion of either the preceding or succeeding curve is out of scale, that is, the calculated relative density is higher than the true density.

CONCLUSION

Punch tilting always occurs in a rotary tablet machine during the compression cycle and should be taken into account together with the machine

deformation. The correct values of punch penetration in the die depend on both phenomena.

Like machine deformation, punch tilting also depends in practice on the compression force used, regardless of the type of material under study. This means that if the device installed in the rotary machine for monitoring punch penetration fails to assess the tilting effect, the phenomenon should be minimised by using compression forces as low as possible for the study of powder densification. This could be achieved by using small size punches (6 mm or below). In any case, even if minimised, punch tilting is always present, and should always be taken into consideration in order to obtain more accurate data. Heckel analysis can be easily and correctly carried out in a rotary machine with the installation of two symmetrical transducers per punch, or with the use of any other device capable of including punch tilting in the evaluation of punch penetration.

REFERENCES

1. Nelson E, Busse LW, Higuchi T. 1955. The physics of tablet compression. VII. Determination of energy expenditure in the tablet compression process. *J Am Pharm Assoc (Sci Ed)* 44:223–225.
2. Heckel RW. 1961. Density-pressure relationships in powder compaction. *Trans Metall Soc AIME* 221: 671–675.
3. Heckel RW. 1961. An analysis of powder compaction phenomena. *Trans Metall Soc AIME* 221:1001–1008.
4. Rees JE, Hersey JA, Cole ET. 1972. Simulation device for preliminary tablet compression studies. *J Pharm Sci* 61:1313–1315.
5. Celik M, Marshall K. 1989. Use of a compaction simulator system in tableting research. *Drug Dev Ind Pharm* 15:759–800.
6. Muller FX, Augsburger LL. 1994. The role of the displacement-time waveform in the determination of Heckel behaviour under dynamic conditions in a compaction simulator and a fully instrumented rotary tablet machine. *J Pharm Pharmacol* 46: 468–475.
7. Palmieri GF, Joiris E, Bonacucina G, Cespi M, Mercuri A. 2005. Differences between eccentric and rotary tablet machines in the evaluation of powder densification behaviour. *Int J Pharm* 298: 164–175.
8. Matz C, Bauer-Brandl A, Rigassi T, Schubert R, Becker D. 1999. On the accuracy of a new displacement instrumentation for rotary tablet presses. *Drug Dev Ind Pharm* 25:117–130.
9. Doelker E. 1994. Assessment of powder compaction. In: Chulia D, Deleuil M, Pourcelot Y, editors. *Powder technology and pharmaceutical process*. Elsevier: Amsterdam, pp 403–471.